

A Fast and Self-Acting Release-Caging-Mechanism for Actively Driven Drop Tower Systems

Andreas Gierse¹  · Ulrich Kaczmarczik¹ · Andreas Greif¹ · Hanns Selig¹ · Peter von Kampen¹ · Thorben Könemann¹ · Claus Lämmerzahl¹

Received: 5 May 2017 / Accepted: 11 September 2017 / Published online: 26 September 2017
© Springer Science+Business Media B.V. 2017

Abstract Today's and future scientific research programs ask for high quality microgravity conditions of 10^{-6} g on ground combined with high repetition rates of 100 flights per day or more. Accordingly, a new type of drop tower, the GraviTower Bremen, (GTB), has been suggested and is currently under development. As a first stage of development, a GTB-Prototype (GTB-Pro) has been designed which uses an active rope drive to accelerate a slider/drag shield and an experiment therein on a vertical parabola. During the free fall phase, the experiment is decoupled from the slider by a self-acting Release-Caging-Mechanism (RCM). Our prototype will provide 2.5 s of microgravity for experiments of up to 500 kg for at least 100 times per day. In this article, the final concept of the engineering of the active rope drive and the RCM are presented in detail. Based on extensive simulations aiming at an optimization of the whole system we developed a hydraulic rope drive system with minimized vibrational amplitude and low number of eigenfrequencies. The RCM achieves a very fast (≤ 0.1 s) self-acting release of the experiment from the slider by making use of the dynamics of the hydraulic rope drive. Furthermore, passive hydraulic stop dampers in the RCM build a passive and self-acting recoupling mechanism. This system is optimized for a fast decoupling to compensate for the time limitation posed by the chosen drive technology. The simulations

included a comparison of different drive technologies, physical effects like the Coriolis force, and the dynamics of the RCM system itself.

Keywords Drop tower · Microgravity · Free-Flyer · Mechanical decoupling

Future Drop Towers

Limitations of Currently Existing Drop Towers

Drop Towers offer many advantages compared to other microgravity facilities: Permanent access to microgravity, easy access to the experiment between drops, very good quality of weightlessness down to $\sim 10^{-6}$ g, and moderate costs are among the most important advantages (Lämmerzahl and Steinberg 2015). At present, only three larger drop towers with weightlessness durations of more than 3 s are operated continuously for scientific experiments. As longer free fall durations result in higher drop velocities of the experiment, all of these systems use some implementation of a vacuum around the experiment in order to avoid aerodynamic drag.

- The Beijing Drop Tower at the National Microgravity Laboratory (NML) offers a free fall distance of 61 m and, thus, reaches duration of 3.5 s of weightlessness (Wan et al. 2010). In normal operation, the experiment capsule is dropped with a surrounding evacuated drag shield and experiences 10^{-5} g of residual quasi-static acceleration. The mass of the experiment is limited to 70 kg.

✉ Andreas Gierse
andreas.gierse@zarm.uni-bremen.de

¹ ZARM, University of Bremen, Am Fallturm, 28359 Bremen, Germany

- The evacuated drop shaft at the NASA Glenn Research Center is 143 m long and offers 5.2 s of weightlessness for an experiment of up to 455 kg (Zero Gravity Research Facility 2017). The highest permissible air pressure inside the drop shaft required to achieve a microgravity quality of $10^{-5} g$ is 2 Pa. The repetition rate is strongly limited due to the evacuation and flooding with dried air.
- The ZARM drop tower in Bremen is also based on the concept of an evacuated drop tube. It became a worldwide unique facility through its catapult system. The catapult, located at the bottom of the tower, accelerates within 0.2 s the capsule with an experiment of a total mass of up to 500 kg to a final velocity of 47 m/s, which thereon moves on a vertical parabola achieving 9.3 s of weightlessness (Dittus 1991). For particularly sensitive experiments the evacuation process can be extended to up to 24 h, giving a residual air pressure of less than 5 Pa. Furthermore, an additional drag shield/Free-Flyer system was developed in order to further increase the microgravity quality to up to $10^{-8} g$. As the drag shield already falls in vacuum, an additional vacuum between drag shield and experiment is not necessary so that the advantage of convection cooling of the electronics within the capsule is kept.

The main overall drawback in the performance of these drop towers is the low repetition rate due to the need for a vacuum. At ZARM a typical number of drops per scientific campaign for one experiment is 15 to 20 performed within two or three weeks (Kufner and et al. 2011). To get enough data points many scientists carry out several campaigns with the same or similar experiments.

In the following this article describes the development of key technologies to achieve good microgravity condition with high repetition rates without vacuum.

Evaluation of Scientist Needs

In 2012 scientists who used the ZARM Drop Tower were asked to specify their overall needs regarding microgravity conditions. It turned out that the most urgent need of the scientists is to be able to perform parameter scans as well as precision measurements based on good statistics. All this requires a large number of drops/flights which can be realized only with drop towers with high repetition rates. The technically possible increase of the repetition rate by a factor of 20 would be a first major step in meeting the needs of the scientific community.

A higher repetition rate would require a higher degree of automation of the performed experiments.

The today's technology is advanced enough to provide an automated control of most of the experiments.

A very important boundary condition to be met is to minimize the oscillations of the experimental structure induced by the initial vertical acceleration process. The excitation of such oscillations can be minimized through a particular strength and form of the acceleration. The evaluation gave that this form has to be sinusoidal and below 5g including a smooth transition from hyper-g to microgravity.

For a wide range of experiments a microgravity duration of 4 s is sufficient. An increasing number of experiments, at the moment 30% of all experiments that were performed at ZARM, used the catapult system to achieve a longer microgravity time. It is clear that for most of the life science experiments even a microgravity duration of 10 s is not sufficient.

According to our 25 years of experience the average experiment mass and volume fitted the existing capsule system at ZARM with 270 kg and 0.45 m³ net weight and volume for the experiment (500 kg total mass). For the development of the GTB and GTB-Pro these measures are kept as reference.

The Concept for a New Type of Drop Tower

In order to determine the most suitable design for a new type of drop tower the main design concepts were compared:

1. Drops vs. vertical parabolas:

A vertical parabola requires a catapult system or linear drive which are technically challenging and complex engines. The advantages are that the height and the maximum velocity for a vertical parabola trajectory are respectively a quarter and a half of those of a simple drop.
2. Vacuum drop tube vs. active drag shield:

A drop tube is a very simple device but its evacuation takes a lot of time while an actively controlled drag shield which is positioned to a fixed distance to the free flying experiment requires sophisticated control technology which still needs to be developed for the GTB.
3. Automated recovery and repositioning of the experiment vs. passive deceleration chamber:

As above, the technically more complex automated system allows higher repetition rates but needs to be developed.
4. Passive or active mechanical damping systems vs. decoupled Free-Flyer

On the one hand, a Free-Flyer offers ideal mechanical decoupling from structural vibrations of the slider and mechanical imperfections of any drive. On the other hand, a Free-Flyer is much more sensitive to imperfections of the decoupling mechanisms because already small initial relative velocities of the free flying

experiment with respect to the slider might lead to impacts into the slider.

These main design concepts have to be discussed with respect to the main performance parameters, which are:

- i. repetition rate
- ii. microgravity duration
- iii. microgravity quality

The key determinants for the effective repetition rate of a drop tower are (a) an overall design that does not rely on a vacuum in any manner (evacuation time) and (b) an automated deceleration unit that includes a self-acting recoupling mechanism which also reorientates the experiment after flight, and prepares it for the next flight.

As the necessary height of the tower increases with the square of the microgravity duration structural vibrations of the building become increasingly problematic. With a simple drop 10 s of microgravity already require 490 m of free fall distance not including the deceleration. Long microgravity durations only get feasible with drop shafts or, as implemented in the Bremen drop tower, with a vertical parabola.

The microgravity quality inside the experiment is mainly influenced and limited by imperfections of the drive, structural vibrations inside the experiment and, if not decoupled by a vacuum acoustical excitation, by vibrating parts inside or outside the experiment. A Free-Flyer design with high internal structural damping is favorable compared to active or passive decoupling mechanisms as it perfectly decouples the experiment from the drive and the structure of the drag shield. The GTB concept combines all of these functions, as will be described below.

In summary of the discussion above the decision was made that the design concept of the GTB includes a rail-guided slider which is accelerated by an active drive. Inside the slider, a Free-Flyer is released and recaged automatically at the beginning and the end of the vertical parabola by a RCM. It is a general feature in such setups that this decoupling mechanism between the free flying experiment and drag shield is crucial. A fast decoupling process can lead to initial relative velocities between the experiment and the drag shield which may result in an early unwanted impact. A slow decoupling process would however reduce the microgravity time. As far as the aerodynamic drag is concerned, the relative velocities between the slider and the Free-Flyer are rather small (< 1 mm/s). Therefore, similar to the Free-Flyer system of the Bremen drop tower, it is intended to omit the vacuum inside the drag shield in order to retain the convection cooling for the experiments. As a consequence, it is expected that the Free-Flyer will experience acoustic excitation that limits the achievable microgravity quality.

For the development of the GTB, a repetition rate of one flight every five minutes (96 flights in 8 h) and a

microgravity duration of 4 s are targeted. Furthermore, the allowed initial acceleration was limited to $5g$. The development of this concept was described in more detail in an earlier publication (Könemann and et al. 2015). The further main developments since 2014 involve the drive and the Release-Caging-Mechanism shown here. The construction of a prototype is currently underway that will provide 2.5 s of microgravity for experiments of up to 500 kg to test these new technologies.

Technical Challenges of the GTB and Their Solutions

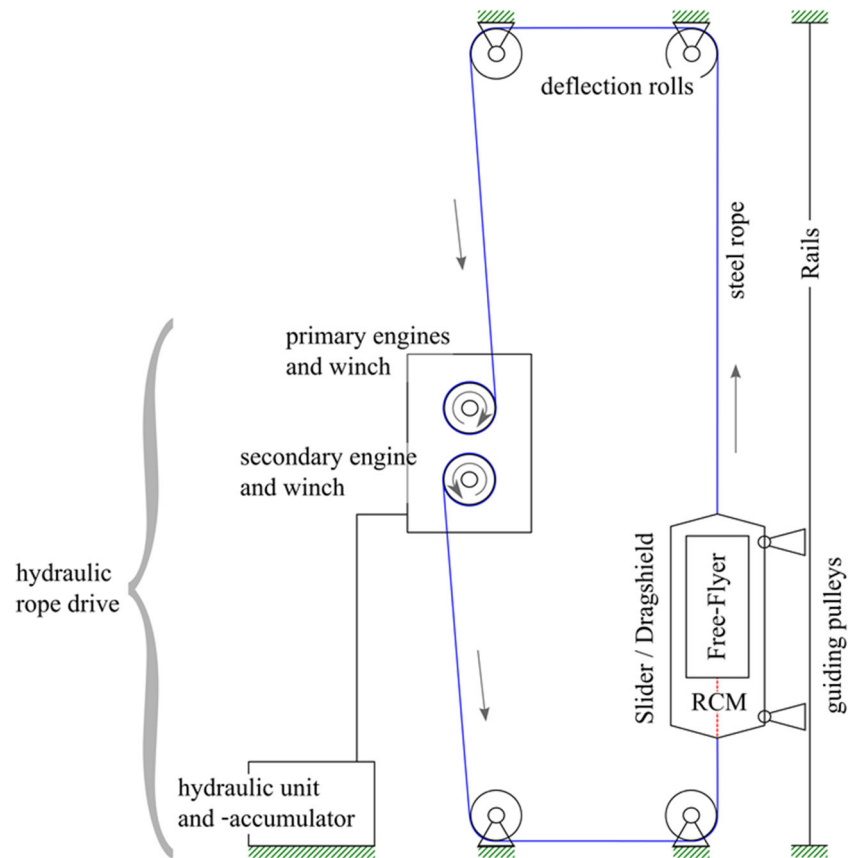
Comparison of Possible Drives

Electro-magnetic drives, like that used for the Transrapid trains, seem to be an ideal drive for an active microgravity platform like the GTB. In 2012 ZARM commissioned a first feasibility analysis on this topic (ThyssenKrupp Transrapid 2012). The main advantages of electromagnetic linear drives are the feasible force vector and dynamics of such systems. It also would be a straightforward and elegant solution to implement eddy-current brakes for the safety concept by short-cutting single drive elements. Despite of all these advantages, additional machinery room is required for the power supply system and for a large number of buffer and recuperation capacitors. Furthermore, the feasibility analysis revealed that the precision of positioning of the slider depends on the size of the electromagnetic dipoles and decreases at low velocities, which occurs at the top dead center. Consequently, the necessary gap size between the Free-Flyer and slider would have to be of the same order of magnitude as the dipole size. The technical realization of the necessary recoupling mechanism for the given size of dipoles was estimated to be highly complex. Therefore, in conclusion of the feasibility analysis we decided to explore alternative drives. Furthermore, the electromagnetic drives turned out to be very expensive.

As second alternative we decided to analyze a hydraulic rope drive concept in collaboration with Bosch-Rexroth, namely a hydraulic rope drive concept based on hydraulic engines and rope-winch.

The primary drive consists of six hydraulic engines which work on one winch. A steel rope is guided via deflection rolls to the top plate of the slider. An additional secondary hydraulic engine tightens the main steel rope by a secondary rope that is connected to the bottom of the slider. This design is necessary in order to achieve the required dynamics. The slider is guided by precision rails, as it also would have been with the electromagnetic drive, as shown in Fig. 1.

Fig. 1 Schematic sketch of the hydraulic rope drive concept



Numerical Simulations of the Hydraulic Rope Drives

In advance of the development of the RCM two simulations were performed by Bosch-Rexroth.

1. The first simulation aimed at a general analysis of the achievable dynamics of such a drive and of a generic system identification.
2. In the second simulation a comprehensive parameter study was performed to optimize the drive for its use in the GTB and to identify residual imperfections of the drive in advance of the RCM development.

A virtual contactless distance sensor measuring the vertical distance between the slider/drag shield and the free flying experiment inside was used as reference sensor in the control loop of the drive. The controller used is not a conventional PID controller but instead an in-house development of Bosch-Rexroth adapted from their hydraulic engines. In this paper we will neither discuss its functioning nor its design, but instead the results of the simulations which show very well the possible adjustments of the controller.

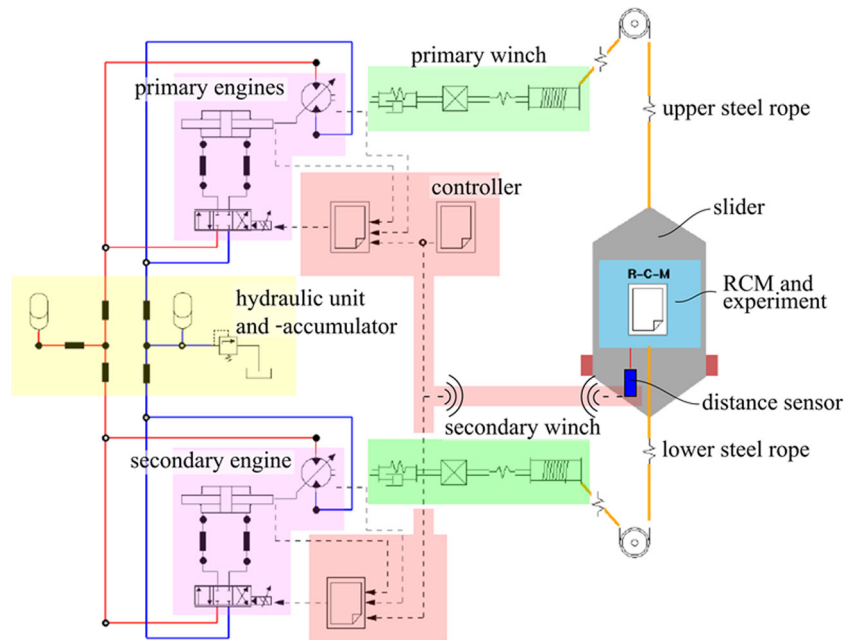
Figure 2 shows an overview of the simulation model including the hydraulic system consisting of the hydraulic accumulator, hydraulic engines and the winches. Furthermore, the arrangement of the ropes, the slider, and the RCM including the experiment are shown. The controller receives

sensor signals from the engines and from the contactless distance sensor.

In the first simulation, a profile with sinusoidal acceleration $a_{\text{dyn}} = 29.34 \text{ m/s}^2$ and a microgravity duration of 2.5 s was chosen as shown in Fig. 3. The black line in the upper part of Fig. 3 shows the target profile while the red line shows the simulated profile that is the system response of the whole setup.

As can be seen from the system response after 0.10 s, the ropes get pretensioned. The combination of the stiffness of the ropes together with the mass of the slider results in a single degree of freedom (SDOF) with an eigenfrequency $f_{e\text{Ropes-Slider}}$ of approximately 13 Hz. This vertical eigenfrequency is clearly visible in the first second of the system response a_{dyn} . At 1 s, after abatement of the oscillation, the acceleration given by the target profile starts and the combination of the simulated engines and the controller shows a dead time of 80 ms. During acceleration, another eigenfrequency at 3.7 Hz dominates. This is the first eigenfrequency of the closed-looped controller $f_{e\text{Controller}}$ which we were able to identify through an additional transfer-function identification of the controller. At the end of the acceleration phase, an overshoot occurs due to the eigenfrequencies and the energy stored in the elastic elongation of the upper steel rope. As this overshoot is highly damped, its effective shape is approximately one period of an oscillation. This result

Fig. 2 The first Bosch-Rexroth numerical simulation model of the GTB drive



was very surprising but welcomed as it leads to an automatic vertical positioning of the Free-Flyer with very low relative velocity several millimeters above its contact surface inside the slider.

Furthermore, see Fig. 3, a Short-Time-Fourier-Transformation (STFT) of the first two seconds of the system response shows the change of the discussed eigenfrequencies as

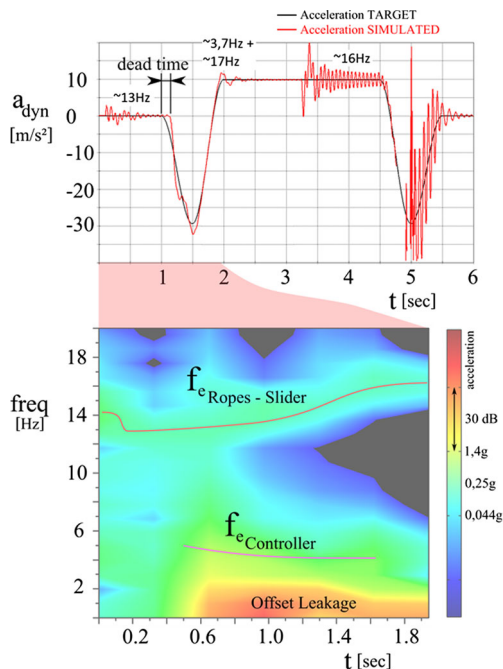


Fig. 3 (above) Acceleration of the slider – targeted (black) and first simulated (red) acceleration. The lower part of the figure shows the Short-Time-Fourier-Transformation (STFT) of the first two seconds

functions of time. The reason for this change is the variable rope strain and length.

After 3.5 s (see Fig. 3), the slider reaches the top dead center where static friction in the engines and guiding pulleys appears. Thus, the vertical eigenfrequency of the setup is excited again. In this simulation the peak at ~ 5 s shows the uncontrolled impact of the Free-Flyer into the slider.

Based on these results of the first simulation it was decided to perform a numerical parameter study as a second simulation step. In order to increase the effective mechanical damping of the two main eigenfrequencies of the drive the design of the controller and the weightings of the different sensor inputs to the controller were varied. Finally, the signal of the distance sensor between slider and experiment was used to minimize this gap by setting up a target profile as shown in Fig. 4.

Furthermore, the targeted acceleration profile was varied during the transition time between acceleration and

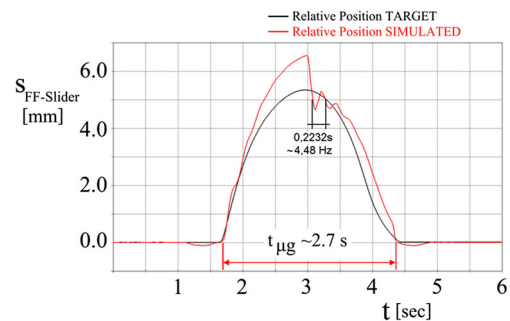


Fig. 4 Relative position of the Free-Flyer to the slider during the vertical parabola

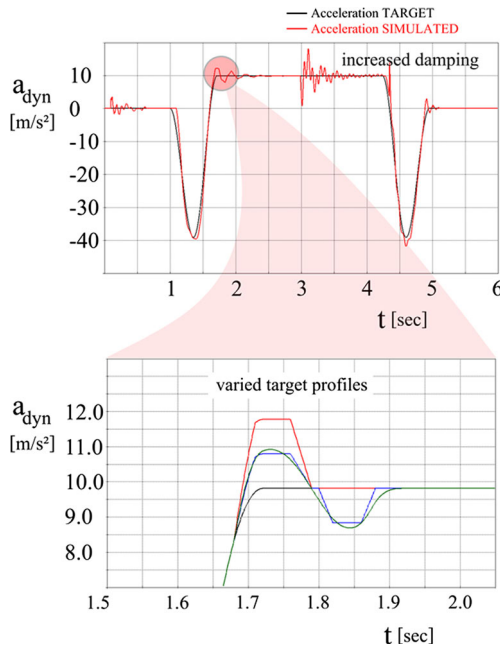


Fig. 5 Optimized damping and varied acceleration profile for the separation of the Free-Flyer in the second simulation

microgravity phase in order to verify the separation of the Free-Flyer from the slider (Fig. 5). The effect of automatic vertical positioning of the Free-Flyer occurred for all target profiles and, thus, it was harnessed for the following developments of the RCM.

The second simulation showed that it is possible to reduce the gap toward the end of the microgravity time down to less than 10 mm (Fig. 5).

These results were harnessed for the following developments of the RCM. Furthermore, as can also be seen from these simulations, a suitably designed hydraulic stop damper could act as an elegant passive recoupling mechanism between the Free-Flyer and the slider.

Based on these results we decided to further develop and use the hydraulic rope drive for the GTB instead of the electro-magnetic drive.

Consideration of Additional Physical Effects on the GTB Design

Weightlessness occurs as a body moves freely and without any external force in a gravitational field. For a spherically symmetric gravitating source for example, the trajectories of a point mass like test body are given by the Keplerian orbits. For the description of the dynamics of bodies on earth which constitutes a non-inertial system, the Coriolis force as well as the centrifugal force have to be taken into account.

These effects depend on the position of the lab on the rotating earth. The position of ZARM is given by the

reference ellipsoid WGS84, the geoid NGA EGM96, and a height above sea level of 5 m to:

$$\begin{pmatrix} x_{ZARM} \\ y_{ZARM} \\ z_{ZARM} \end{pmatrix} = \begin{pmatrix} 3774.8846 \\ 588.2937 \\ 5090.2793 \end{pmatrix} km$$

For simplification, the Earth and its gravitational field are at first considered to be perfectly spherical. In Fig. 6, the position of the GTB at 53.1105° latitude and 8.858° longitude and a not to scale parabola are shown.

Coriolis Force

For a perfectly spherical Earth model without inhomogeneities of local mass distributions, the eastern deflection s_c of a dropped object is caused entirely by the first order Coriolis acceleration (Tiersten and Soodak 2000). In the following the deflection during a vertical parabola is calculated. The Coriolis acceleration is described by

$$\vec{a}_c = 2 \cdot \vec{v} \times \vec{\omega}_0$$

with the Earth’s rotation rate of the sidereal day

$$\omega_0 = 7.292 \cdot 10^{-5} \frac{rad}{s}$$

and the velocity of a free falling object which can be described with

$$\vec{v} = \vec{v}(t) = \vec{g}_0 \cdot t + \vec{v}_0$$

using the effective gravitational acceleration \vec{g}_0 and the initial velocity for the vertical parabola \vec{v}_0 one gets for the Coriolis acceleration

$$\vec{a}_c(t) = 2 \cdot (\vec{g}_0 \cdot t + \vec{v}_0) \times \vec{\omega}_0$$

For the specific case of the GTB the vector notation can be avoided: we assume that the initial velocity is vertical, that is, in direction of the effective gravitational acceleration

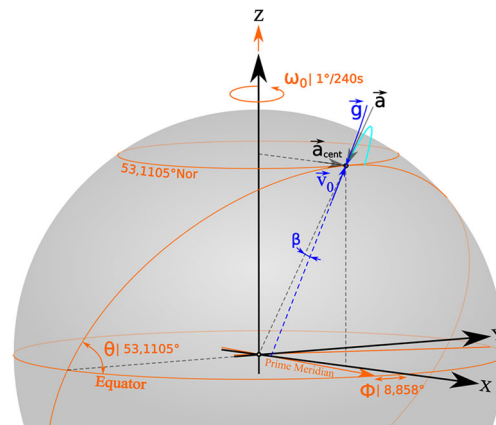


Fig. 6 Position of the GTB on Earth with scaled parabola

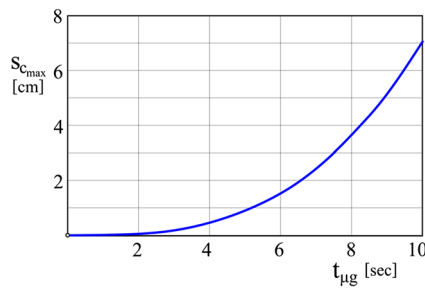


Fig. 7 Total western deflection $s_{c_{max}}$ due to Coriolis acceleration after vertical parabola of duration $t_{\mu g}$

but *negative* (opposite direction). In this case the Coriolis acceleration points westwards (right-hand-rule)

$$a_c(t) = 2 \cdot \omega_0 \cdot \sin(90^\circ - \theta) \cdot (g_0 \cdot t + v_0)$$

where θ is the latitude and $\sin(90^\circ - \theta) = \cos(\theta)$. Twice temporal integration gives the Coriolis deflection for vertical parabola to

$$s_C(t) = \omega_0 \cdot \cos(\theta) \cdot \left[\frac{1}{3} \cdot g_0 \cdot t^3 + v_0 \cdot t^2 \right]$$

Expressing the negative vertical take-off velocity v_0 as function of the microgravity duration $t_{\mu g}$

$$v_0(t_{\mu g}) = \frac{-g_0 \cdot t_{\mu g}}{2}$$

one finally obtains the total deflection at the end of the parabola as function of the microgravity duration as follows

$$s_{C_{max}}(t_{\mu g}) = \omega_0 \cdot \cos(\theta) \cdot \left[\frac{-1}{6} \cdot g_0 \cdot t_{\mu g}^3 \right]$$

as shown in Fig. 7. In the chosen coordinate system the calculated negative values indicate a deflection in westerly direction.

This western deviation leads to a second order Coriolis deflection to the north which is neglected since it is of second order in the Earth rotation and, thus, much smaller.

Centrifugal Deviation

As can be seen in Fig. 6 the initial vertical velocity v_0 of the experiment is aligned to the plumb line given by the effective gravitational field, \vec{g} . The effective gravitational field results from the superposition of the gravitational field, \vec{a} , which points to the earth center and the centrifugal acceleration.

$$a_{cent} = x_{ZARM} \cdot \omega_0^2 = 2.032 \cdot 10^{-2} \frac{m}{s^2}$$

The angle β between gravitational field and effective gravitational field at sea level is very small and defines the necessary alignment accuracy of the rails:

$$\beta_{GTB} = 0.095^\circ$$

Since the centrifugal acceleration depends von the distance from the earth rotation axis, the superposition with the radial field lines of the gravitational field results in curved effective gravity field lines. Tiersten and Soodak calculated the residual deviation due to this curvature of the effective field lines for a dropped object to five times greater than that due to the second order Coriolis Effect. They also refined the model to a spheroidal, flattened Earth which reduced the southern deviation by approximately 20%. Using a non-smooth topography of the gravitational field due to local mass distributions may however lead to a deflection one magnitude greater. The tidal fields of the Moon and Sun on the Earth are in the magnitude of sub micro-*g*. Those of all other external attractors are even smaller. The first order Coriolis effect is by far the greatest physical effect on the free flying experiment. For the development of the GraviTower it was decided to take into account a deviation in the magnitude of the first order Coriolis effect in both horizontal degrees of freedom. Furthermore, as the mechanical imperfections cannot be predicted precisely, it was decided to add a technically feasible extra margin and to make the decoupling mechanism symmetric in positive and negative directions. Based on the shown simulations, the required gaps of the Free-Flyer relative to the slider were defined as ± 40 mm for the horizontal translational degrees of freedom and ± 80 mm for the vertical. All rotational degrees of freedom need at least $\pm 2^\circ$ of free rotation. Furthermore, to avoid mutual interferences between the subsystems, a low-est tolerable eigenfrequency of 30 Hz was defined for the slider.

Development of a Fast and Self-Acting Release-Caging-Mechanism

Earlier Developments for Free-Flyer Systems

The most simple design of a Free-Flyer system, as used in a standard atmosphere environment, incorporates a passive drag shield that encloses the experiment. Both are released simultaneously and start to move with respect to each other as the experiment falls freely and the drag shield is decelerated by the air drag. After the free fall the drag shield is decelerated and the experiment is aligned to it by limit stops.

The Free-Flyer used in the Bremen drop tower, (Fig. 8), falls inside the vacuum chamber at a technically feasible vacuum of 15 Pa. The deceleration of the drag shield in the

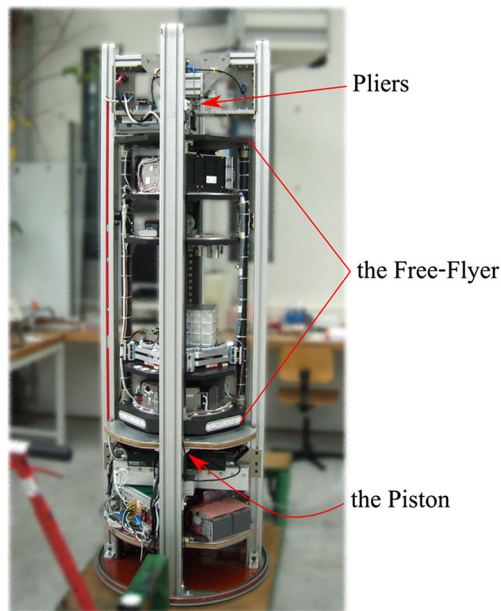


Fig. 8 The Free-Flyer of the Bremen drop tower

Bremen drop tower is comparably small, $2 \cdot 10^{-6} g$, but the deceleration after the free fall reaches up to 400 m/s^2 , and a rebound due to the stiffness of the deceleration unit occurs. The impact of the experiment on the limit stops of the drag shield would result in even higher accelerations and the rebound could lead to uncontrolled bounces. Therefore, in order to protect the experiments from high loads, the Free-Flyer of the Bremen drop tower uses an active decoupling and recoupling mechanism. This mechanism consists of two pairs of pliers fixing a tap of the Free-Flyer at its top and a vertical piston at the bottom.

Directly after the release of the capsule the first pliers at the top are opened and the piston at the bottom is driven downwards. As final step in the decoupling routine, the second, smaller pliers at the top are opened laterally.

In general we observed an influence of the opening speed of the pliers on the initial velocity of the Free-Flyer relative to the drag shield. This relative velocity becomes larger for

larger opening speeds. A total opening time of less than one second regularly led to a lateral impact of the Free-Flyer into the drag shield. In order to avoid these high initial relative velocities it is crucial that both contact surfaces of the pliers are very clean and share identical properties. Even the slightest static friction, due to dirt or grease, pulls the Free-Flyer to one side (Selig and Lämmerzahl 2010). For the GraviTower with its rather short microgravity time it is important to employ a very fast mechanism without any tendency to induce initial velocities into the Free-Flyer. Such a mechanism is what we are going to describe in the next subsections.

The Novel RCM Concept: Fast, Passive, and Automated

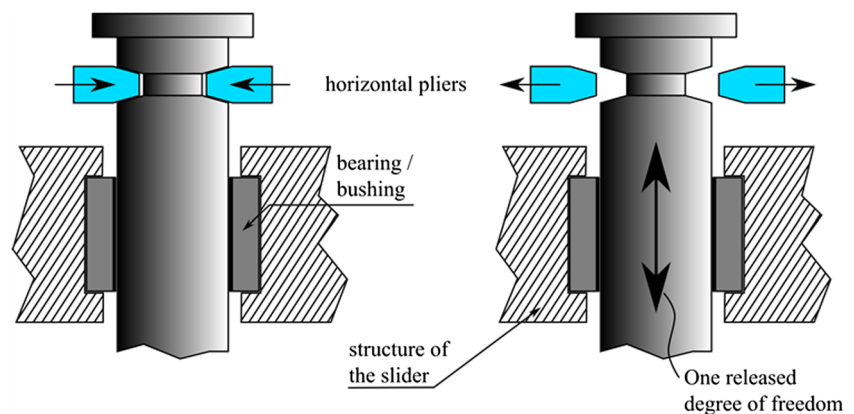
The novel concept of the RCM is based upon a stack of single stage decoupling mechanisms where each degree of freedom is released by its own decoupling mechanism. The fixing pliers open in normal direction to the degree of freedom under consideration. Any horizontal mechanical forces by the pliers are compensated by the bearings which allow motion in the respective degree of freedom only.

Figure 9 shows a schematic of such a decoupling system for the vertical translational degree of freedom. A bearing bush creates the vertical degree of freedom but absorbs all horizontal translational forces and, if necessary, also all moments.

A stack of such mechanisms represents a decoupling mechanism with six degrees of freedom. As all pliers can be opened simultaneously and imperfections do not cause relevant relative velocities, the opening process can be very short. Consequently, between opening and recaging we get a perfectly freely flying experiment while the effective gaps are always just the bearings clearances; this also makes the recaging process very short.

The use of plain bearings with very good slipping properties allows to release five degrees of freedom already during the phase of vertical acceleration. Only the vertical translational degree of freedom cannot be set free

Fig. 9 RCM concept of the new decoupling mechanism



during acceleration. This allows the decoupling process to be extremely fast.

The experiment, with a height of 1.5 m, is positioned above the RCM like a tumbler. The center of rotation for the rotational degrees of freedom around the horizontal axes is located slightly above the experiment’s center of gravity as can be seen in Fig. 10. This creates a restoring moment against rotational disturbances during the acceleration time and, thus, an automatic repositioning before flight. The rotational degree of freedom around the z-axis is released simultaneously but is not affected by the vertical acceleration.

Also the horizontal translational degrees of freedom are released at the end of the acceleration phase to minimize the influence of imperfections of the guiding rails. The vertical translational degree of freedom uses the overshoot of the drive for an automatic vertical positioning of the Free-Flyer as described above and is released at last at the end of the acceleration phase and the beginning of the microgravity phase. As all three translational degrees of freedom cannot reposition themselves using gravity they have to be repositioned by an additional pneumatic system between the flights.

Despite the simple fundamental concept the final design of the whole RCM is very complex. A detailed explanation of the design is beyond the scope of this publication.

Limit Stops for the Free-Flyer

If a translational or rotational deviation exceeds the gaps of the RCM, then the Free-Flyer must be halted and recoupled to the slider by hard limit stops with the consequence that the experiment cannot be carried through. Based on the expected/calculated motions of the Free-Flyer relative to the

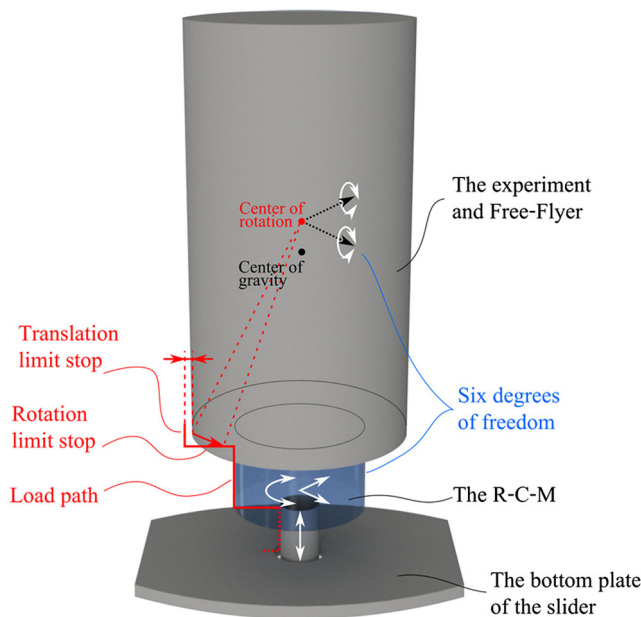


Fig. 10 Principle of the limit stops

drag-shield it has to be decided whether it is possible to use a Free-Flyer system or to employ as alternative system an active or passive reposition system during the flight.

As first alternative to a Free-Flyer system passive soft limit-stops possessing spring and damper characteristics would give small restoring forces which are proportional to the deviation. Such soft limit stops could be used in order to limit the effects of initial relative velocities. Consequently, the necessary total gap size could be reduced and hitting of the Free-Flyer into the drag shield could easily be avoided. The severe disadvantages of this setup are the vibrations and transient distortions that are transmitted through the soft limit stops during free fall.

A second alternative are active repositioning systems, which would virtually increase the effective dynamic mass of the Free-Flyer or virtually lower the effective stiffness of the isolators. The expected transient distortions and high relative velocities inside the GTB are beyond the range of application of all existing active systems. The typical application for active isolation systems are long-duration tests that make use of decoupling frequencies below 1/100 Hz (Grodsinsky and Whorton 2000).

Based on these considerations, it was decided to keep the gaps in the RCM as calculated above and not to use active or passive repositioning systems. Hard rubber limit-stops and appropriate load paths surrounding the RCM were designed as shown in Fig. 10.

Final Numerical Simulation of the RCM

Finally, a multibody-model of the experiment, the RCM, and the slider was developed, see Fig. 11, and has been added to the previous simulation model.

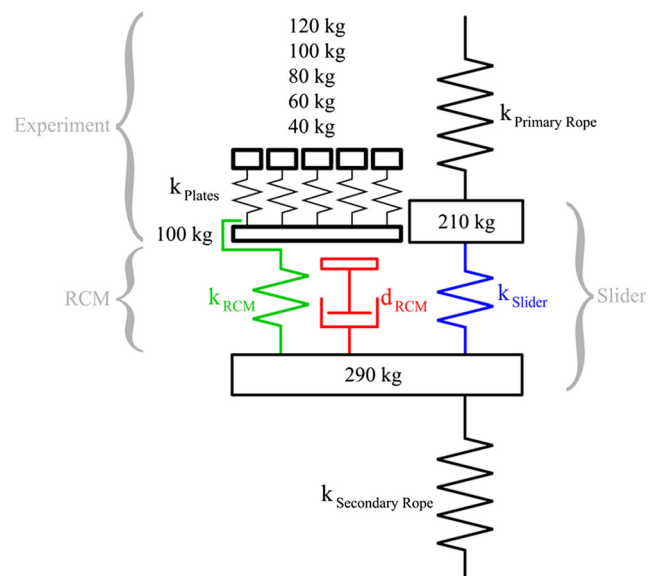


Fig. 11 Substitute model of the experiment, the RCM and the slider

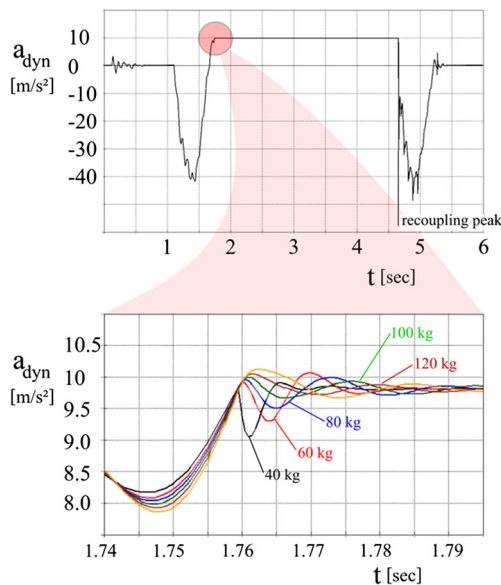


Fig. 12 Acceleration of the Free-Flyer and the plates (40 kg–120 kg)

Since it was decided to keep the design of the Bremen drop tower experiments for the GTB, the experiment platform consists of four vertical stringers and several mounting plates for housing the experiment itself, as can be seen in Fig. 8. For the simulation we use five mounting plates with equal stiffness k_{Plates} , and experiment masses on top varying from 40 kg to 120 kg. The stiffness of the RCM between slider and experiment was calculated from the CAD model of the RCM and described by k_{RCM} in the simulation. The damper with the damping parameter d_{RCM} represents the hydraulic stop damper for the recoupling process with an initial gap to the experiment during microgravity time.

For the simulation, the slider was modeled by two nodal points with 210 kg mass at the top and 290 kg mass at the bottom. Between these two nodal points the vertical stiffness of the slider k_{Slider} as calculated from a CAD model was considered.

Figure 12 shows the acceleration of the free flying experiments with five plates with different experiment masses on top during one complete parabola. The mechanical energy stored in the structure of the Free-Flyer due to the initial vertical acceleration leads to an abating ringing after the acceleration phase. This disturbing effect is well known from the existing catapult system in the Bremen drop tower where it is reduced by mounting plates with high inertial damping. At the end of the microgravity phase an acceleration peak due to the recoupling impact of the Free-Flyer on the hydraulic stop dampers d_{RCM} of approximately 6g was calculated. This acceleration is considerably smaller than the impact peak in the deceleration-chamber of the Bremen drop tower, and is mechanically harmless for all experiments.

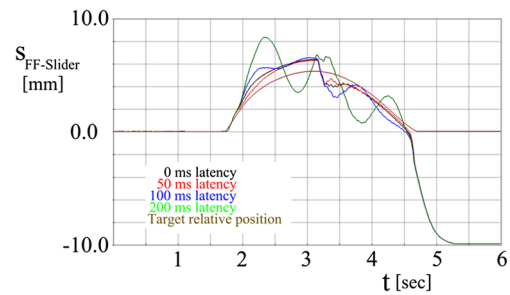


Fig. 13 Effect of sensor latency on the closed loop controller of the drive

Since these results were really promising we investigated in addition hidden risks in technical subsystems as the radio path of the reference sensor, the size of the hydraulic accumulator, the friction in the hydraulic engines, and atmospheric conditions. For instance, the impact of the latency of the radio path of the reference position sensor signal from the slider to the control center on the whole system has been estimated by a simulation employing varying latencies, see Fig. 13. With increasing latency the closed loop controller exhibits an oscillation tendency starting at approximately 100 ms of latency.

For this as for all other investigated issues on technical subsystems technical solutions were found or developed. To sum up, no obstruction to the functionality of the system has been found.

Construction and Design of the RCM

We come out with the final results of our simulations.

As discussed above, the size and mass of the experiments for the GTB were kept the same as the ones for the Bremen

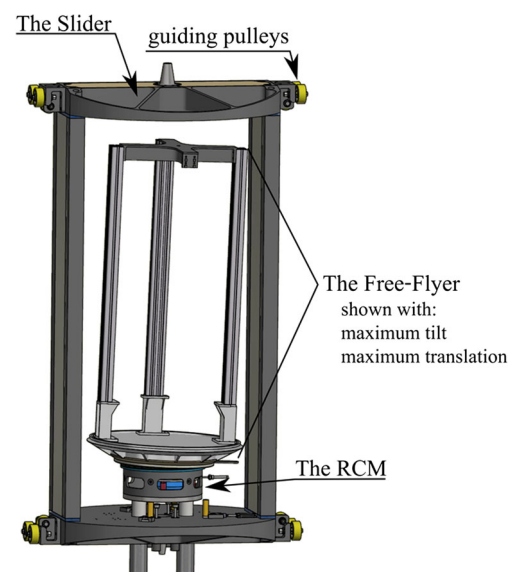
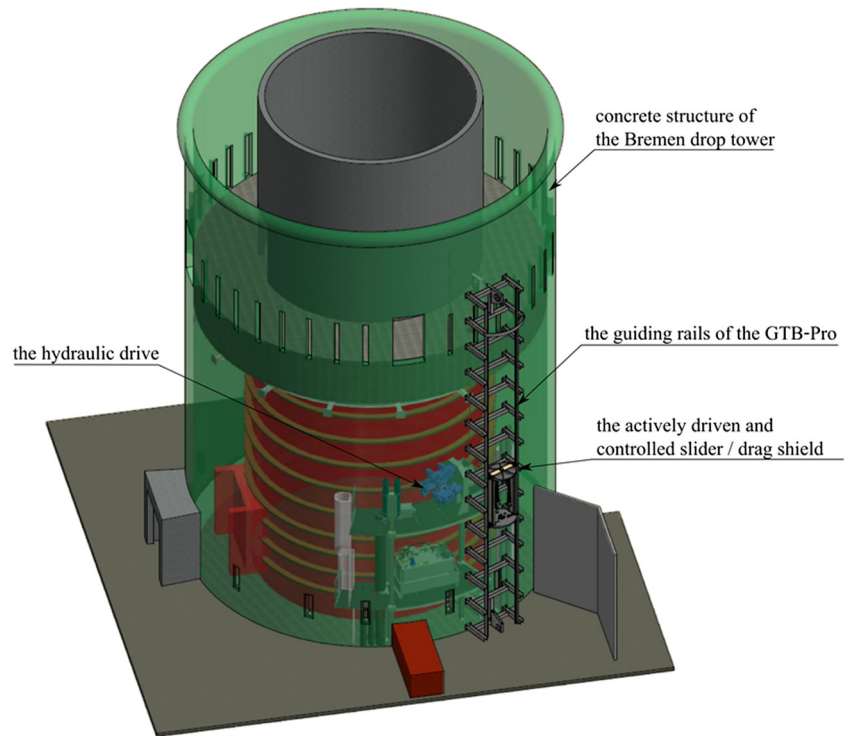


Fig. 14 The slider with RCM and Free-Flyer

Fig. 15 The GTB-Pro at the Bremen drop tower



drop tower with the advantage of having full compatibility between both facilities.

Figure 14 shows the slider/drag shield without its doors and the RCM and Free-Flyer inside. The doors of the slider are aerodynamically tight but not gas tight. Inside the slider, the free flying experiment moves in the standard atmosphere to ensure the possibility of convectional cooling for the experiment. The rigid symmetrical design of the slider is necessary in order to minimize asymmetric deformations during acceleration since the clearances of the bearings in the RCM are very tight and, thus, sensitive to deformations.

The RCM makes the experiment a real Free-Flyer with the advantage of full mechanical decoupling from the structure of the slider and the imperfections of the drive. It is possible to combine some degrees of freedom without violating the described RCM concept. The developed RCM combines the desired properties of a very fast decoupling and recoupling of the free flying experiment and an automated reorientation of the Free-Flyer between two flights.

Hard rubber stops limit the free deflection in all degrees of freedom. If one of these limits is reached during microgravity time, the experiment is prematurely stopped and will have to be repeated.

The impact forces and moments are carried over to the slider by specially designed load paths parallel to the stacked decoupling mechanisms of the RCM. For the recoupling procedure shock absorbers and hydraulic dampers catch the Free-Flyer and align it to the motion of the slider. The maximum acceleration during recoupling is limited to 10g.

The novel design of the RCM is generic and might be used for other drop towers as well.

The Building

The overall height of the GTB-Pro is 14.9 m so that it fits inside the existing ZARM integration hall. Figure 15 shows a CAD model of the ground floor with the lower section of the Drop Tower. On the left hand side, the entrance to the tower can be seen. At the top, we have the drop tube of the tower which was cut for simplification. The rails and the slider of the GTB-Pro can also be seen in the front. The drive is completely hidden as it will be mounted behind the wall. The ropes will therefore be guided through the wall by deflection wheels. As the GTB-Pro will be part of the ZARM integration hall it will be easily and quickly accessible for experiments. The control center for the whole system will be placed directly next to the rails.

Conclusion and Outlook

For a proof of concept of the GraviTower Bremen, a Prototype (GTB-Pro) providing 2.5 s of microgravity, is currently being constructed. The presently main engineering developments of the GTB-Pro are the hydraulic rope drive and the RCM. The development and simulation of the rope drive was realized in collaboration between Bosch-Rexroth and

ZARM. The technical challenge of very fast opening and closing times for the decoupling mechanisms was resolved by inventing a new design with separate mechanisms for the different degrees of freedom. Both developments reached their final stages in 2016 and the production of the initial components started later that year. The assembly and tests of the subsystems will take place in 2017; commissioning of the GTB-Pro is planned for 2018. After that, the first experiments will be automated to put the possible repetition rate into practice. The achieved microgravity quality will be monitored and, if necessary, adjustments on structural damping and noise canceling will be made.

The experience gained through running experiments will also lead to new guidelines for the experiments and handling the huge amount of experimental data. If the GTB-Pro fulfills the expectations, the development of the GTB, which will provide 4 s of microgravity, will start. For the GTB an additional umbilical system to supply the experiment might be added to the RCM design.

Acknowledgements ZARM gratefully acknowledges the support for the Bremen drop tower and the funding of the VibraMIK project (grant number 50WF1302) from the DLR Space Administration.

We gratefully thank our colleagues Mr. Maik Schulze, Mr Stephan Karl, Mr. Tobias Gottsmann, Mr. Christoph Rüb and Mr. Jens Rückel from Bosch-Rexroth for the excellent collaboration in the GTB-Pro project.

We like to thank our colleagues at ZARM, University of Bremen for their support during the whole project.

Acronyms

GTB	Gravi Tower Bremen
GTB-Pro	Gravi Tower Bremen - Prototype
NML	National Microgravity Laboratory in Beijing

PID	Proportional Integral Derivative (controller)
RCM	Release Caging Mechanism
SDOF	Single Degree of Freedom
STFT	Short Time Fourier transform
ZARM	Center of Applied Space Technology and Microgravity
μg	Microgravity

References

- Dittus, H.: Drop Tower Bremen: a weightlessness laboratory on Earth. *Endeavour, New Series* **15**(2), 72–78 (1991)
- Grodsinsky, CM., Whorton, MS.: A survey of active vibration isolation systems for microgravity applications. NASA Technical Report (2000)
- Könemann, T., et al.: Concept for a next-generation drop tower system. *Adv. Space Res.* **55**, 1728 (2015)
- Kufner, E., et al.: ESA's drop tower utilisation activities 2000 to 2011. *Microgravity Sci. Technol.* **23**, 409–425 (2011)
- Lämmerzahl, C., Steinberg, T.: Drop Towers. In: Beysens, D.A., van Loon, J.J.W.A. (eds.) *Generation and Applications of Extra-Terrestrial Environments on Earth*. River Publishers Series in Standardization, p. 45. River Publishers, Aalborg and Delft (2015)
- ThyssenKrupp Transrapid: GraviTower Bremen (GTB) Linearantrieb, unpublished (2012)
- Tiersten, MS., Soodak, H.: Dropped objects and other motions relative to the noninertial earth. *Am. J. Phys.* **68**, 129–142 (2000)
- Selig, H., Lämmerzahl, C.: Drop tower microgravity improvement towards the nano-g level for the MICROSCOPE payload tests. *Microgravity Sci. Technol.* **22**, 539–549 (2010)
- Wan, S.H., Yin, M.G., Guan, X.D., Lin, H., Xie, J.C., Hu, W.R.: Drop Tower Beijing and short-time microgravity experiments. In: 38th COSPAR Scientific Assembly, Drop Tower Days (G0.2), Germany (2010)
- Zero Gravity Research Facility: NASA Glenn Research Center, USA.-Fact Sheet, <<http://facilities.grc.nasa.gov/documents/TOPS/TopZERO.pdf>> (2017)